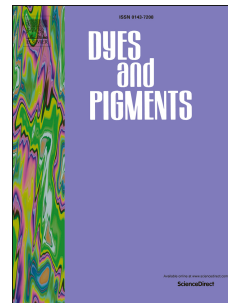


Accepted Manuscript

Novel organic dyes with anchoring group of Quinoxaline-2, 3-diol and the application in dye-sensitized solar cells

Lei Wang, Xichuan Yang, Xiuna Wang, Licheng Sun



PII: S0143-7208(14)00378-7

DOI: [10.1016/j.dyepig.2014.09.019](https://doi.org/10.1016/j.dyepig.2014.09.019)

Reference: DYPI 4532

To appear in: *Dyes and Pigments*

Received Date: 3 June 2014

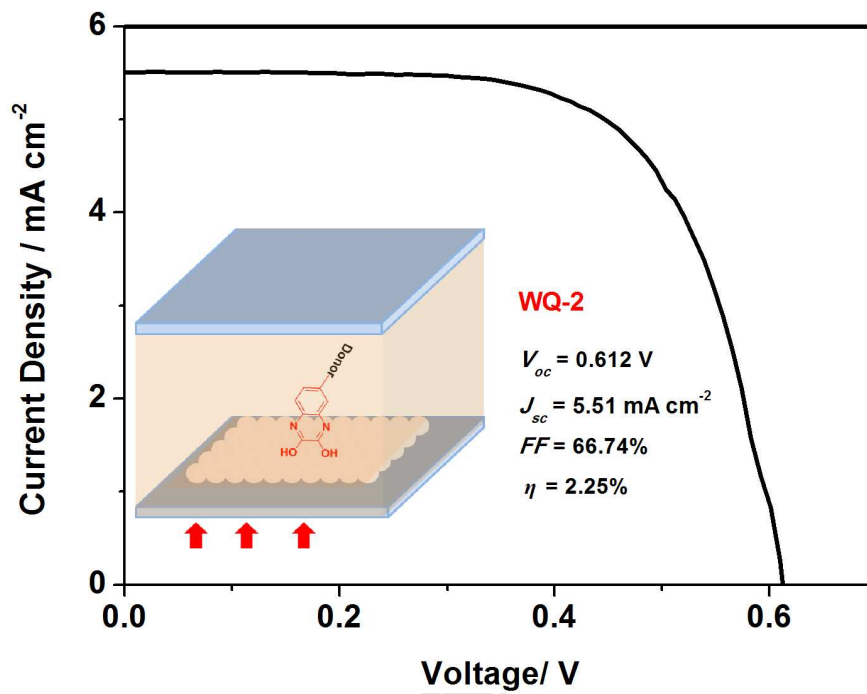
Revised Date: 7 September 2014

Accepted Date: 9 September 2014

Please cite this article as: Wang L, Yang X, Wang X, Sun L, Novel organic dyes with anchoring group of Quinoxaline-2, 3-diol and the application in dye-sensitized solar cells, *Dyes and Pigments* (2014), doi: 10.1016/j.dyepig.2014.09.019.

This is a PDF file of an unedited manuscript that has been accepted for publication. As a service to our customers we are providing this early version of the manuscript. The manuscript will undergo copyediting, typesetting, and review of the resulting proof before it is published in its final form. Please note that during the production process errors may be discovered which could affect the content, and all legal disclaimers that apply to the journal pertain.

Graphical Abstract for Paper



Novel Organic Dyes with Anchoring Group of Quinoxaline-2, 3-diol and the Application in Dye-sensitized Solar Cells

Lei Wang,^a Xichuan Yang,^{*a} Xiuna Wang^a and Licheng Sun^{a,b}

^a State Key Laboratory of Fine Chemicals, Dalian University of Technology (DUT), DUT-KTH
Joint Education and Research Center on Molecular Devices, Dalian 116024, China.

^b Department of Chemistry, School of Chemical Science and Engineering, KTH Royal Institute
of Technology, 100 44 Stockholm, Sweden.

* E-mail: yangxc@dlut.edu.cn; Fax: (+86) 411-84986250

ABSTRACT: Two organic quinoxaline dyes (**WQ-1** and **WQ-2**) with a structure of quinoxaline-2, 3-diol as the electron withdrawing and anchoring group were synthesized and applied in the dye-sensitized solar cells. Fourier transform infrared spectroscopy and two other reference dyes (**WQ-R1** and **WQ-R2**) without the hydroxyl groups were introduced to ascertain the adsorption properties of the dye series. The effect of the new electron acceptor and anchoring group on the performance of solar cells was investigated systematically. Under the standard light illumination (100 mW m^{-2}), **WQ-2** got an efficiency of 2.25%, with a short circuit photocurrent density of 5.51 mA cm^{-2} , an open circuit voltage of 0.612 V and a fill factor of 66.74%.

KEY WORDS: DSSCs; organic sensitizers; quinoxaline-2, 3-diol; anchoring group; FTIR

INTRODUCTION

Due to the tremendous energy demands today, dye-sensitized solar cells (DSSCs) which were first developed by O'Regan and Grätzel in 1991^[1] have drawn much attention during the past three decades.^[2-4] The main components of a DSSC are photoanode, electrolyte and counter electrode. The photoanode is composed of conductive electrode coated with a semiconductor material that is sensitized with dye molecules which absorb the sunlight and transfer their excited electrons to the conduction band of the semiconductor.^[8-16]

For organic sensitizers with hydroxyl as anchoring group, owing to the special direct one-step electron injection from the dyes to TiO₂ by photo-excitation of the dye-to-TiO₂ charge-transfer bands (DTCT),^[17-20] the energy loss decreases which is beneficial to improve the efficiency of DSSCs. The representative dye sensitizers often employ catechol, phenol and their derivatives as anchoring groups in the dye structures. An et al. reported a class of thiophene-catechol light harvesting molecules used in DSSCs and the efficiency was 0.76%.^[21] Tae further improved the efficiency to about 1.6% also with catechol as anchoring group.^[22] A traditional D- π -A structure was introduced with 2-hydroxybenzotrile as the electron acceptor/anchoring unit in our group and the best efficiency was about 3.4%.^[23] With colourless sulfur/iodide-based hybrid electrolyte, the sensitizers with hydroxypyridium unit reported by Zhao et al. got an efficiency of 2.6%.^[24] The efficiency is not very high mainly because the fast electron recombination and the narrow absorption spectra of type II sensitizers.^[25]

Therefore one strategy to improve the performance is to modify the structure of type II organic sensitizers, especially for the anchor group. As a common structure used as the pesticide and raw material for industrial synthesis, quinoxaline has been applied in organic sensitizers as electron withdrawing bridge which successfully broadens the spectra response.^[26-28] In this work, one of its derivatives quinoxaline-2, 3-diol with enediol structure was introduced as a new type of

anchoring group in the type II dye molecules to further strengthen the electron withdrawing property and further improve the absorption spectra. Triphenylamine was introduced as the donor part, and the structures of **WQ-1** and **WQ-2** were shown in Figure 1.

EXPERIMENTAL SECTION

General Synthetic Procedure

As shown in Scheme 1, both dyes were synthesized according to the traditional methods including amino group protection and deprotection reaction, Suzuki reaction, N-alkylation coupling reaction. MS data were obtained with GC-TOF MS (UK), HP1100 LC/MSD (USA), and LC/Q-TOF MS (UK). ^1H NMR spectra were taken with VARIAN INOVA 400MHz (USA) using TMS as standard. Commercial reagents and solvents were used as received without further purification.

di-tert-butyl(4-bromo-1,2-phenylene)dicarbamate (1). 4-bromobenzene-1, 2-diamine (3.74 g, 20 mmol) and di-tert-butyl dicarbonate (9.34 g, 43 mmol) were dissolved in 100 mL ethanol and stirred for 8 h at room temperature. The solvent was then evaporated and the crude product was purified by column chromatography using CH_2Cl_2 /hexane (v/v, 1/3) to get compound **1** as a white solid (7.36 g, yield 95%). **1:** ^1H NMR (400 MHz, Acetone- d_6) δ 8.00 (d, $J = 12.7$ Hz, 2H), 7.87 (s, 1H), 7.49 (d, $J = 8.6$ Hz, 1H), 7.26 (dd, $J = 8.7, 2.3$ Hz, 1H), 1.48 (s, 18H). TOF HRMS-EI(m/z) calcd. for $\text{C}_{16}\text{H}_{23}\text{N}_2\text{O}_4\text{Br}$ [M^+] 386.0841, found 386.0838.

4-(Diphenylamino)phenylboronic acid (2). To a 100 mL two necked flask containing a solution of 4-bromotriphenylamine (7.13 g, 22 mmol) in dried THF (50 mL), $^n\text{BuLi}$ (10.8 mL, 27 mmol, 2.5 M) was added slowly at -78°C under N_2 while stirring. After stirring for 1 h at -78°C , trimethyl borate (3.2 mL, 27 mmol) was added into the solution and maintained at -78°C for

1 h. After stirring at room temperature for another 8 h, water was added to quench the reaction mixture and diluted HCl (2 M) was added until an acidic mixture was obtained. The reaction mixture was poured into water and extracted with CH₂Cl₂ (3 × 50 mL). The combined organic layer was dried with anhydrous Na₂SO₄ and evaporated to dryness. The crude product was purified by column chromatography using CH₂Cl₂/ethyl acetate (v/v, 1/1) as eluent. The boronic acid compound **2** was obtained as a white solid (4.90 g, yield 76%). **2**: ¹H NMR (400 MHz, DMSO-d₆) δ 7.88 (s, 2H), 7.67 (d, *J* = 8.3 Hz, 2H), 7.30 (t, *J* = 7.8 Hz, 4H), 7.10 – 6.98 (m, 6H), 6.88(d, *J* = 8.3 Hz, 2H).

di-tert-butyl(4'-(diphenylamino)-[1,1'-biphenyl]-3,4-diyl)dicarbamate (3). A mixture of compound **1** (2.71 g, 7 mmol), compound **2** (2.08 g, 7.2 mmol), THF (80 mL), K₂CO₃ aqueous solution (2 M, 5 mL), and Pd(PPh₃)₄ (50 mg, 0.05 mmol) was degassed and charged with N₂. The mixture was stirred at 70 °C for 8 h. The reaction mixture was poured into water and extracted with ethyl acetate (3 × 50 mL). The combined organic layers were dried with anhydrous Na₂SO₄ and evaporated. The residue was purified by column chromatography using CH₂Cl₂/hexane (v/v, 1/1) to afford **3** as a yellow solid (3.24 g, yield 84%). **3**: ¹H NMR (400 MHz, Acetone-d₆) δ 8.00 (s, 2H), 7.87 (s, 1H), 7.62 (d, *J* = 8.4 Hz, 1H), 7.60 – 7.54 (m, 2H), 7.40 (dd, *J* = 8.4, 2.2 Hz, 1H), 7.36 – 7.28 (m, 4H), 7.14 – 7.04 (m, 8H), 1.51 – 1.50 (m, 18H). TOF HRMS calcd. for C₃₄H₃₇N₃O₄ [M⁺] 551.2784, found 551.2791.

WQ-1. To a 100 mL two necked flask with compound **3** (1.66 g, 3 mmol) in 20 mL CH₂Cl₂ solution, 2 mL trifluoroacetic acid in 10 mL anhydrous CH₂Cl₂ was added slowly and stirred at room temperature for 4 h. Then 50 mL H₂O was added into the reaction solution, white solid was precipitated and filtered. After dried at 50 °C for 2 h, 1 equiv Oxalic acid dihydrate was added and grinded in mortar for 20 min. The mixture was added into an autoclave with teflon lining

under N₂ and heated at 170 °C for 6 h. After cooled into room temperature, the solid was dissolved and purified by column chromatography using CH₂Cl₂/CH₃OH (v/v, 50/1) to afford **WQ-1** as a pale yellow solid (0.24 g, yield 21%). **WQ-1**: ¹H NMR (400 MHz, DMSO-d₆) δ 11.96 (s, 2H), 7.50 (d, *J* = 8.1 Hz, 2H), 7.33 (t, *J* = 7.4 Hz, 6H), 7.18 (d, *J* = 8.2 Hz, 1H), 7.05 (d, *J* = 8.1 Hz, 8H). TOF HRMS calcd. for C₂₆H₁₉N₃O₂ [M⁺] 405.1477, found 405.1481.

N, N-diphenyl-4-(thiophen-2-yl) aniline (4). 4-bromotriphenylamine and thiophen-2-yl boronic acid were reacted as reaction **c** to get the white compound **4** (yield 81%). **4**: ¹H NMR (400 MHz, Acetone-d₆) δ 7.60 – 7.55 (m, 2H), 7.40 – 7.35 (m, 2H), 7.35 – 7.29 (m, 4H), 7.12 – 7.02 (m, 9H). TOF HRMS calcd. for C₂₂H₁₇NS [M⁺] 327.1082, found 327.1072.

N, N-diphenyl-4-(5-(4, 4, 5, 5-tetramethyl-1, 3, 2-dioxaborolan-2-yl)thiophen-2-yl) aniline (5). To a solution of **2** (0.794 g, 2.43 mmol) in THF (50 mL), ⁿBuLi (1.17 mL, 2.5 M in n-hexane) was added dropwisely at –78 °C under N₂. The reaction was kept at –78 °C for 1 h. Then 2-isopropoxy-4, 4, 5, 5-tetramethyl-1, 3, 2-dioxaborolane (0.456 g, 2.45 mmol) was added, the mixture was allowed to warm to room temperature and stirred overnight. The solution was extracted with ether, and the combined organic layers were dried over anhydrous Na₂SO₄ and evaporated to dryness. The residue was purified by chromatography on silica gel eluting with hexane/ethyl acetate (v/v, 20/1) to afford **5** as a yellow solid (0.77 g, 70%). **5**: ¹H NMR (400MHz, CDCl₃) δ 7.63 – 7.52 (m, 1H), 7.39 – 7.28 (m, 5H), 7.19 – 7.03 (m, 10H), 1.38 (s, 12H). GC/TOF HRMS-EI (m/z): [M]⁺ calcd. for C₂₈H₂₈NO₂SB, 453.1934; found, 453.1939.

di-tert-butyl (4-(5-(4-(diphenylamino)phenyl)thiophen-2-yl)-1,2-phenylene)dicarbamate (6). Compound **5** and compound **1** were reacted as reaction **c** to get the yellow solid **6** (yield 70%). **6**: ¹H NMR (400 MHz, Acetone-d₆) δ 8.02 (s, 2H), 7.93 (s, 1H), 7.65 – 7.59 (m, 3H), 7.45 (dd, *J* = 8.4, 2.2 Hz, 1H), 7.38 (d, *J* = 2.2 Hz, 3H), 7.33 (dd, *J* = 8.5, 7.4 Hz, 3H), 7.14 – 7.08 (m,

6H), 7.06 (d, $J = 8.7$ Hz, 2H), 1.51 (t, $J = 4.8$ Hz, 18H). TOF HRMS calcd. for $C_{38}H_{39}N_3O_4S$ [M+] 633.2661, found 633.2670.

WQ-2: **WQ-2** was gained by compound **6** by a similar reaction as **WQ-1**. **WQ-2:** 1H NMR (400 MHz, DMSO- d_6) δ 11.96 (d, $J = 26.2$ Hz, 2H), 7.59 (d, $J = 8.7$ Hz, 2H), 7.43 (d, $J = 1.8$ Hz, 1H), 7.42 – 7.36 (m, 2H), 7.34 (t, $J = 7.9$ Hz, 5H), 7.16 (d, $J = 8.4$ Hz, 1H), 7.08 (dd, $J = 12.7, 7.4$ Hz, 6H), 6.99 (d, $J = 8.7$ Hz, 1H). TOF HRMS calcd. for $C_{30}H_{21}N_3O_2S$ [M+] 487.1354, found 487.1366.

Preparation of Dye-sensitized Solar Cells

The DSSCs were fabricated as follows. A double-layer TiO_2 photoelectrode (thickness 14 μm , area 6 \times 6 mm) was used as a working electrode. Fluorine-doped tin oxide (FTO) glass plates (Pilkington-TEC8) were cleaned using an ultrasonic bath by detergent and ethanol each for 30 min. A layer of 10 nm TiO_2 paste (T/SP, SALARONIX) was coated on the FTO glass by screen printing and then dried for 3 min at 130 $^\circ C$. This procedure was repeated for 6 times to get a 10 μm film, then a 4 μm layer of 300 nm (DHS-SLP1, Heptachroma, China) TiO_2 paste was screen-printed as scattering layer. The double-layer TiO_2 electrodes were gradually heated under an air flow to 500 $^\circ C$ and maintained for 30 min. The sintered film was further treated with 40 mM $TiCl_4$ aqueous solution at 70 $^\circ C$ for 30 min, then washed with water and ethanol, and annealed at 500 $^\circ C$ for 30 min. After the film was cooled to 80 $^\circ C$, it was immersed into a 2×10^{-4} M dye solution in a mixed solvent of ethanol and dichloromethane (v/v, 4/1) under dark for 10 h. Co-sensitization was done in a solution with 2×10^{-4} M dye and 0.5 equiv, 1.0 equiv CDCA in the solution, respectively. The sensitized TiO_2 electrode was then rinsed with the ethanol and dried. The hermetically sealed cells were fabricated by assembling the dye-loaded film as the working electrode and sintered Pt/FTO counter electrode (Heptachroma, China) separated with a hot-melt

Surlyn 1702 film (60 μm , Dupont). Electrolyte consisting of 0.3 M 1, 2-dimethyl-3-n-propylimidazolium iodide (DMPII), 0.25 M LiI, 0.01 M I_2 , 0.05 M tetrabutyl ammonium iodide (TBAI), 0.1 M 4-terbutyl pyridine in acetonitrile/valeronitrile (AN/VN = 85/15, v/v) was injected into the cell and sealed with a cover glass.

Prepared solar cells were characterized by current–voltage characteristics (J - V) and incident photon-to-current conversion efficiency (IPCE). Current–voltage characteristics were carried out with an AM 1.5G solar simulator (Newport, UK). The incident light intensity was 1000 W m^{-2} calibrated with a standard Si solar cell. For the J - V curves, the active area was 0.1256 cm^2 . The measurement of the incident photon-to-current conversion efficiency (IPCE) was performed by a Hypermono-light (SM-25, Jasco Co. Ltd., Japan). The J_{sc} was calibrated by integrating the IPCE value tuned light density of AM 1.5 against wavelength.

RESULTS AND DISCUSSION

The UV-Vis absorption spectra of **WQ-1** and **WQ-2** were collected and displayed in Figure 2. Considering the dissolving property of the dye series, a mixed solvent of ethanol and dichloromethane (v/v, 4/1) was chosen in this work. The UV-Vis absorption spectra of the **WQ** dye solution and the dye-adsorbed transparent TiO_2 films (T/SP, SOLARONIX, doctor-blade printed on a clean glass, sensitized 1 h in dye bath) were recorded on a HP8453 (USA) spectrophotometer. In the solution, owing to the simple conjugation system of the dye series, the absorption spectra of both dyes were cutted off at 450 nm. Compared with other similar dye structures, existence of the heterocyclic ring in the acceptor unit increased the electron withdrawing property and the absorption maxima was red-shifted further.^[23] For **WQ-1**, the maximum absorption peak was at 346 nm, after the introduction of thiophene to increase the conjugation system and ease the spatial tension, the absorption of **WQ-2** in the solution was red-

shifted for about 35 nm and the extinction coefficient increased to $2.81 \times 10^4 \text{ M}^{-1} \text{ cm}^{-1}$. After adsorbed on the TiO_2 film, although the peak for **WQ-1** is affected by the noise of blank spectra of TiO_2 film, the absorption peaks became broader clearly and were extended to about 500 nm. The color of dyed films was apparently darker than that of the dye solution which was also showed in the inset photograph. The interaction between dye molecules and TiO_2 surface leads to the aggregation and the form of DTCT band, and both consequently, broaden the absorption spectra that have been gained. ^[20, 26]

Chenodeoxycholic acid (CDCA) has been broadly employed as a co-adsorbent to make the arrangement of dye molecules on the TiO_2 surface more orderly. ^[29, 30] To further investigate adsorption properties, UV-Vis spectra of the **WQ** dyes on the film co-adsorbed with CDCA were also collected and showed in Figure 3. The absorption peaks of both dyes were red-shifted with the addition of CDCA in the dye solution. Previous studies showed after DTCT bands were formed by adsorbed on the TiO_2 , the LUMO levels were decreased accordingly, which caused the red-shift of the UV-Vis spectra. Through the increase of CDCA, the aggregation was suppressed continuously, the peaks were narrowed ^[31-33] and this trend became more obvious.

Electrochemical redox potentials were showed in Figure 4. The energy levels of **WQ** dyes were determined by cyclic voltammetry (CV) and the corresponding data were also collected in Table 1. The data were obtained using a three-electrode cell by the electrochemistry workstation (CHI630, CHINA). The working electrode was a glass carbon disk electrode, the auxiliary electrode was a Pt wire, and Ag/Ag^+ was used as the reference electrode. Tetrabutylammonium hexafluorophosphate was used as supporting electrolyte in $\text{CH}_2\text{Cl}_2/\text{CH}_3\text{CH}_2\text{OH}$ (v/v, 1/4). The ferrocenium/ferrocene (Fc/Fc^+) redox couple was used as an internal potential reference also showed in Figure 4. Table 1 showed photo-electrical property of the quinoxaline-2, 3-diol dyes.

The ground state oxidation potentials *vs.* NHE were calibrated by addition of 440 mV to the potentials *vs.* Fc/Fc⁺, which were sufficiently positive compared to the redox potential of the I/I₃⁻ couple (0.35 V *vs.* NHE) as an electrolyte. Additionally the estimated LUMO levels of both dyes were much more negative than the conduction-band edge of TiO₂ (-0.5 V *vs.* NHE), ensuring an efficient electron injection process from the excited state of dye molecules into the conduction band of TiO₂. The expansion of π -conjugated system of **WQ-2** decreased the energy gap between HOMO and LUMO. Furthermore, the large difference between the TiO₂ conductive band and the LUMO levels of the dyes suggested that 4-*tert*-butylpyridine could be used in the electrolyte to yield a higher photo-voltage.

The energy state and electron distribution were calculated to gain insight into the photoelectrical properties of **WQ** dye series. The structural and electronic properties of the dyes were calculated with DFT (density functional theory) at the B3LYP/6-31G (d) level in gas phase using the Gaussian 09 program package, TD-SCF methods were introduced to calculate the energy of excitation state. The optimized geometries and isodensity plots of the frontier orbitals of the chromospheres were shown in Table S1. Indicated by the calculation results, the HOMO was mostly located on the triphenylamine and π -bridge moiety, the LUMO was mostly located on the quinoxaline-2, 3-diol moiety. It was also clear that the HOMO and LUMO localized more reasonable for **WQ-2** owing to the introduction of thiophene. Compared with the unbounded states, the calculations of electron densities showed that the photostimulated exciton (LUMO density) was localized more on the Ti-hydroxyl chelate site in the adsorbed **WQ** dyes, which was a proof of DTCT band.^[20, 21] The energy calculation result also proved the narrow down of energy levels after the adsorption of **WQ** dyes, which will cause the absorption red-shifted and is in accordance with the experimental result.

The FTIR spectra of dye powder and the dye-loaded TiO₂ powder were collected by the FTIR equipment (NEXUS, America) and the results were showed in Figure 5. The TiO₂ films were immersed into the dye solutions overnight in the dark, dried and scraped off the glass to form the samples. To collect the spectra of dye powder, KBr was chosen to be a blank. For the dyed TiO₂ powder, the spectra were recorded with TiO₂ as a blank. As we have known, quinoxaline-2, 3-diol had two resonant structures—"keto" form and "enolic" form. After the synthesis was finished, no further treating method was introduced, and the NMR data illustrated the structure of the dye series were in the "enolic" form. Confirmed by checking the library of FTIR spectra,^[34] here FTIR showed again the same result, as the stretching vibration of hydroxyl group appeared at about 3500 cm⁻¹, the peak at 1270 cm⁻¹ was the stretching vibration of C-O bond in hydroxyl group. Peaks at about 1690 cm⁻¹, 1590 cm⁻¹, 1470 cm⁻¹ were assigned to the skeleton vibration of aromatic structures. There was little change for the benzene skeleton after adsorbed on the TiO₂, but for the C=N stretching vibration peaks at 1690 cm⁻¹, the wavenumber was decreased and shifted to around 1620 cm⁻¹, which could indicate the existence of relation between the nitrogen and TiO₂,^[35-38] or it was caused by the change of electronic effect after adsorption of O-H on TiO₂.

To determine which interaction caused this change, we also synthesized two other reference dyes **WQ-R1** and **WQ-R2** without the hydroxyl groups, the structures were showed in Figure 6 and the synthesis details were summarized in Scheme S1 in the supporting information. Unexpectedly, although both dyes with or without steric hindrance displayed better photo absorption properties in the solution, there was no adsorption phenomena observed on the TiO₂ film by UV-Vis equipment after immersing the TiO₂ film into the reference dye solution for

more than 48 h. So the shifts of C=N vibration peaks were caused mainly by change of electronic effect and **WQ** dyes were adsorbed by the hydroxyl groups.

The dye series were fabricated into the DSSCs then to investigate the photovoltaic properties. The J - V curves of both dyes were collected and showed in Figure 7, all the data were summarized in Table 2. The efficiency for **WQ-1** and **WQ-2** were 1.18% and 1.58% respectively, mainly because of the low short circuit photocurrent density (J_{sc}). CDCA were introduced to co-sensitize with the **WQ** dye, and the consistency of CDCA in the sensitizing solution was changed to optimize the performance. When the molar ratio was 1/0.5 (Dye/CDCA), both dyes gained the best efficiency. Under the optimal condition, for **WQ-1** the highest open circuit voltage (V_{oc}) was 0.662 V, because of the narrow light absorption range, a J_{sc} of 4.10 mA cm⁻² was gained, with a fill factor (FF) of 69.5%, the eventual efficiency was 1.89%. **WQ-2** got a higher J_{sc} of 5.51 mA cm⁻² owing to the extended light absorption response, although V_{oc} decreased to 0.612 V, a better efficiency of 2.25% was gained eventually. The further increase of CDCA didn't improve the performance because competitive adsorption between dye molecules and CDCA was not beneficial for the solar cells. Figure 6b showed the IPCE curves of the solar cells co-adsorbed by **WQ** dye and CDCA. For the comparatively narrow absorption range, IPCE responses were cutted at about 600 nm, and the summit of IPCE curves was about 73% got by **WQ-2** at 420 nm. Considering the comparatively low extinction efficient of **WQ** dyes, the electron injection efficiency was high.

The electrochemical impedance spectroscopy (EIS) also was employed to study the interfacial charge transfer processes in DSSCs based on the **WQ** dyes. EIS tests were carried out using an impedance/gain-phase analyzer (Zennium Zahner, German) with forward bias under dark. The spectra were scanned in a frequency range of 10⁻²-10⁶ Hz at room temperature. The alternate

current (AC) amplitude was set at 10 mV, under dark conditions with an applied bias voltage of -0.680 V. This result was collected in Figure 8. The intermediate frequency semicircle in the Nyquist plot represents the charge transfer phenomena between the TiO₂ surface and the electrolyte.^[39] This recombination resistance decreased in the order of **WQ-1** > **WQ-2**. Additionally the electron recombination lifetimes (τ) were calculated from the angular frequency (ω_{min}) at the intermediate-frequency peak in bode phase plot using $\tau = 1/\omega_{min}$. The calculation results showed the same order as the recombination resistance. Co-sensitization of CDCA on the surface of TiO₂ further helped to increase the recombination resistance of the solar cells, for **WQ** dyes, the addition of 0.5 equiv CDCA was the best condition in Figure 7, which was in consistence with performance of the solar cells.

CONCLUSION

Two organic dye sensitizers with quinoxaline-2, 3-diol were synthesized and applied into the dye-sensitized solar cells. As a new electron acceptor and anchoring group, quinoxaline-2, 3-diol showed a good electron withdrawing property and the absorption of dyes red-shifted compared with the other similar dye molecules without heterocyclic ring. FTIR study showed that **WQ** dyes were adsorbed by hydroxyl groups, which was also proved by the reference dyes without hydroxyl groups. Overall the **WQ** dyes showed comparatively good performance given their simple structures. Under the standard light illumination (AM 1.5G, 100 mW cm⁻²), **WQ-2** got an efficiency of 2.25%, with $J_{sc} = 5.51 \text{ mA cm}^{-2}$, $V_{oc} = 0.612 \text{ V}$, $FF = 66.74\%$ and the IPCE value reached 73%.

APPENDIX Supporting Information

Supporting information includes the synthetic routes of reference dyes and the gaussian caculation result of the **WQ** dyes.

ACKNOWLEDGEMENT

We gratefully acknowledge the financial support of this work from China Natural Science Foundation (Grant 21276044, 21120102036, 91233201, 51372028), the National Basic Research Program of China (Grant No. 2014CB239402), the Swedish Energy Agency, K&A Wallenberg Foundation.

REFERENCE

- [1] O'Regan B, Gratzel M. A low-cost, high-efficiency solar cell based on dye-sensitized colloidal TiO₂ films. *Nature*. 1991;353(6346):737-40.
- [2] Yella A, Lee H-W, Tsao HN, Yi C, Chandiran AK, Nazeeruddin MK, et al. Porphyrin-Sensitized Solar Cells with Cobalt (II/III)-Based Redox Electrolyte Exceed 12 Percent Efficiency. *Science*. 2011;334(6056):629-34.
- [3] Yum JH, Baranoff E, Kessler F, Moehl T, Ahmad S, Bessho T, et al. A cobalt complex redox shuttle for dye-sensitized solar cells with high open-circuit potentials. *Nature communications*. 2012;3:631.
- [4] Mathew S, Yella A, Gao P, Humphry-Baker R, Curchod BF, Ashari-Astani N, et al. Dye-sensitized solar cells with 13% efficiency achieved through the molecular engineering of porphyrin sensitizers. *Nature chemistry*. 2014;6(3):242-7.
- [5] Hagfeldt A, Boschloo G, Sun L, Kloo L, Pettersson H. Dye-sensitized solar cells. *Chemical reviews*. 2010;110(11):6595-663.
- [6] Hao F, Dong P, Luo Q, Li J, Lou J, Lin H. Recent advances in alternative cathode materials for iodine-free dye-sensitized solar cells. *Energy & Environmental Science*. 2013;6(7):2003-19.
- [7] Wang M, Gratzel C, Zakeeruddin SM, Gratzel M. Recent developments in redox electrolytes for dye-sensitized solar cells. *Energy & Environmental Science*. 2012;5(11):9394-405.
- [8] Delcamp JH, Yella A, Holcombe TW, Nazeeruddin MK, Gratzel M. The molecular engineering of organic sensitizers for solar-cell applications. *Angewandte Chemie*. 2013;52(1):376-80.
- [9] Maggio E, Martsinovich N, Troisi A. Using orbital symmetry to minimize charge recombination in dye-sensitized solar cells. *Angewandte Chemie*. 2013;52(3):973-5.

- [10] Handa S, Wietasch H, Thelakkat M, Durrant JR, Haque SA. Reducing charge recombination losses in solid state dye sensitized solar cells: the use of donor-acceptor sensitizer dyes. *Chem Commun (Camb)*. 2007(17):1725-7.
- [11] Kinoshita T, Dy JT, Uchida S, Kubo T, Segawa H. Wideband dye-sensitized solar cells employing a phosphine-coordinated ruthenium sensitizer. *Nature Photonics*. 2013;7(7):535-9.
- [12] Yum JH, Holcombe TW, Kim Y, Rakstys K, Moehl T, Teuscher J, et al. Blue-coloured highly efficient dye-sensitized solar cells by implementing the diketopyrrolopyrrole chromophore. *Scientific reports*. 2013;3:2446.
- [13] Balasingam SK, Lee M, Kang MG, Jun Y. Improvement of dye-sensitized solar cells toward the broader light harvesting of the solar spectrum. *Chemical Communications*. 2013;49(15):1471-87.
- [14] Holliman PJ, Davies ML, Connell A, Vaca Velasco B, Watson TM. Ultra-fast dye sensitisation and co-sensitisation for dye sensitized solar cells. *Chem Commun (Camb)*. 2010;46(38):7256-8.
- [15] Mishra A, Fischer MK, Bauerle P. Metal-free organic dyes for dye-sensitized solar cells: from structure: property relationships to design rules. *Angewandte Chemie*. 2009;48(14):2474-99.
- [16] Preat J, Jacquemin D, Perpète EA. Towards new efficient dye-sensitised solar cells. *Energy & Environmental Science*. 2010;3(7):891.
- [17] Blackburn RL, Johnson CS, Hupp JT. Surface intervalence enhanced Raman scattering from ferrocyanide on colloidal titanium dioxide. A mode-by-mode description of the Franck-Condon barrier to interfacial charge transfer. *Journal of the American Chemical Society*. 1991;113(3):1060-2.
- [18] Ghosh HN, Asbury JB, Weng Y, Lian T. Interfacial Electron Transfer between Fe(II)(CN)₆⁴⁻ and TiO₂ Nanoparticles: Direct Electron Injection and Nonexponential Recombination. *The Journal of Physical Chemistry B*. 1998;102(50):10208-15.
- [19] Khoudiakov M, Parise AR, Brunshwig BS. Interfacial Electron Transfer in Fe(II)(CN)₆⁴⁻-Sensitized TiO₂ Nanoparticles: A Study of Direct Charge Injection by Electroabsorption Spectroscopy. *Journal of the American Chemical Society*. 2003;125(15):4637-42.

- [20] Ooyama Y, Yamada T, Fujita T, Harima Y, Ohshita J. Development of D- π -Cat fluorescent dyes with a catechol group for dye-sensitized solar cells based on dye-to-TiO₂ charge transfer. *Journal of Materials Chemistry A*. 2014;2(22):8500.
- [21] An B-K, Hu W, Burn PL, Meredith P. New Type II Catechol-Thiophene Sensitizers for Dye-Sensitized Solar Cells. *The Journal of Physical Chemistry C*. 2010;114(41):17964-74.
- [22] Tae EL, Lee SH, Lee JK, Yoo SS, Kang EJ, Yoon KB. A Strategy To Increase the Efficiency of the Dye-Sensitized TiO₂ Solar Cells Operated by Photoexcitation of Dye-to-TiO₂ Charge-Transfer Bands. *The Journal of Physical Chemistry B*. 2005;109(47):22513-22.
- [23] Li S-F, Yang X-C, Cheng M, Zhao J-H, Wang Y, Sun L-C. Novel D- π -A type II organic sensitizers for dye sensitized solar cells. *Tetrahedron Letters*. 2012;53(27):3425-8.
- [24] Zhao J, Yang X, Cheng M, Li S, Sun L. Molecular Design and Performance of Hydroxypyridium Sensitizers for Dye-Sensitized Solar Cells. *ACS Applied Materials & Interfaces*. 2013;5(11):5227-31.
- [25] Kaniyankandy S, Verma S, Mondal JA, Palit DK, Ghosh HN. Evidence of Multiple Electron Injection and Slow Back Electron Transfer in Alizarin-Sensitized Ultrasmall TiO₂ Particles. *The Journal of Physical Chemistry C*. 2009;113(9):3593-9.
- [26] Yang J, Ganesan P, Teuscher J, Moehl T, Kim YJ, Yi C, et al. Influence of the Donor Size in D- π -A Organic Dyes for Dye-Sensitized Solar Cells. *Journal of the American Chemical Society*. 2014;136(15):5722-30.
- [27] Pei K, Wu Y, Islam A, Zhang Q, Han L, Tian H, et al. Constructing High-Efficiency D-A- π -A-Featured Solar Cell Sensitizers: a Promising Building Block of 2,3-Diphenylquinoxaline for Antiaggregation and Photostability. *ACS Applied Materials & Interfaces*. 2013;5(11):4986-95.
- [28] Chang DW, Lee HJ, Kim JH, Park SY, Park S-M, Dai L, et al. Novel Quinoxaline-Based Organic Sensitizers for Dye-Sensitized Solar Cells. *Organic Letters*. 2011;13(15):3880-3.
- [29] Yeh-Yung Lin R, Lin H-W, Yen Y-S, Chang C-H, Chou H-H, Chen P-W, et al. 2,6-Conjugated anthracene sensitizers for high-performance dye-sensitized solar cells. *Energy & Environmental Science*. 2013;6(8):2477.
- [30] Lopez-Duarte I, Wang M, Humphry-Baker R, Ince M, Martinez-Diaz MV, Nazeeruddin MK, et al. Molecular engineering of zinc phthalocyanines with phosphinic acid anchoring groups. *Angewandte Chemie*. 2012;51(8):1895-8.

- [31] Lee Y-G, Park S, Cho W, Son T, Sudhagar P, Jung JH, et al. Effective Passivation of Nanostructured TiO₂ Interfaces with PEG-Based Oligomeric Coadsorbents To Improve the Performance of Dye-Sensitized Solar Cells. *The Journal of Physical Chemistry C*. 2012;116(11):6770-7.
- [32] de Miguel G, Marchena M, Ziótek M, Pandey SS, Hayase S, Douhal A. Femto- to Millisecond Photophysical Characterization of Indole-Based Squaraines Adsorbed on TiO₂ Nanoparticle Thin Films. *The Journal of Physical Chemistry C*. 2012;116(22):12137-48.
- [33] Ziótek M, Karolczak J, Zalas M, Hao Y, Tian H, Douhal A. Aggregation and Electrolyte Composition Effects on the Efficiency of Dye-Sensitized Solar Cells. A Case of a Near-Infrared Absorbing Dye for Tandem Cells. *The Journal of Physical Chemistry C*. 2013;118(1):194-205.
- [34] Pouchert CJ. *The Aldrich library of FT-IR spectra*: Aldrich Milwaukee, WI, 1997.
- [35] Ooyama Y, Inoue S, Nagano T, Kushimoto K, Ohshita J, Imae I, et al. Dye-sensitized solar cells based on donor-acceptor pi-conjugated fluorescent dyes with a pyridine ring as an electron-withdrawing anchoring group. *Angewandte Chemie*. 2011;50(32):7429-33.
- [36] Ooyama Y, Yamaguchi N, Imae I, Komaguchi K, Ohshita J, Harima Y. Dye-sensitized solar cells based on D-[small pi]-A fluorescent dyes with two pyridyl groups as an electron-withdrawing-injecting anchoring group. *Chemical Communications*. 2013;49(25):2548-50.
- [37] Greijer H, Lindgren J, Hagfeldt A. Resonance Raman Scattering of a Dye-Sensitized Solar Cell: Mechanism of Thiocyanato Ligand Exchange. *The Journal of Physical Chemistry B*. 2001;105(27):6314-20.
- [38] Shi C, Dai S, Wang K, Pan X, Kong F, Hu L. The adsorption of 4-*tert*-butylpyridine on the nanocrystalline TiO₂ and Raman spectra of dye-sensitized solar cells in situ. *Vibrational Spectroscopy*. 2005;39(1):99-105.
- [39] Adachi M, Sakamoto M, Jiu J, Ogata Y, Isoda S. Determination of Parameters of Electron Transport in Dye-Sensitized Solar Cells Using Electrochemical Impedance Spectroscopy. *The Journal of Physical Chemistry B*. 2006;110(28):13872-80.

Captions for Figures, Schemes and Tables

Table 1 Photophysical and electrochemical properties of **WQ-1**, **WQ-2** dyes

Table 2 Photovoltaic performance of DSSCs based on **WQ-1**, **WQ-2** dyes

Scheme 1 Synthetic routes of **WQ** dyes

Figure 1 The structures of dyes **WQ-1**, **WQ-2**

Figure 2 The absorption spectra of **WQ-1**, **WQ-2** in ethanol and dichloromethane (v/v, 4/1) solution (a) and on the TiO₂ films (b); inset is the photograph of the solutions and films (c)

Figure 3 The absorption spectra of **WQ-1** (a), **WQ-2** (b) on the films co-adsorbed with CDCA

Figure 4 CV curves of **WQ** dyes

Figure 5 FTIR spectra of **WQ-1** and **WQ-2** dye powder and dye on the TiO₂

Figure 6 The structures of reference dyes **WQ-R1**, **WQ-R2**

Figure 7 The *J-V* curves (a) and IPCE spectra (b) of DSSCs based on **WQ-1**, **WQ-2** dyes

Figure 8 The Nyquist (a) and Bode (b) plots of DSSCs based on **WQ-1** and **WQ-2**

Table 1. Photophysical and electrochemical properties of **WQ-1**, **WQ-2** dyes

Dye	λ_{max} (nm)	ε ($\times 10^4$ $M^{-1}cm^{-1}$)	λ_{max} on TiO_2 (nm)	HOMO ^a (V vs. NHE)	E_{0-0} ^b (V)	LUMO (V vs. NHE)
WQ-1	346	2.61	350	0.824	2.93	-2.10
WQ-2	382	2.81	370	0.776	2.74	-1.96

^a The oxidation potentials of the dyes were measured and converted to NHE by addition of 440 mV. ^b E_{0-0} was determined from intersection of the tangent of absorption on TiO_2 film and the X axis by $1240/\lambda$.

Table 2 Photovoltaic performance of DSSCs based on **WQ-1, WQ-2** dyes

Dye	CDCA	V_{oc}	J_{sc}	FF	η
		(mV)	(mA/cm ²)	(%)	(%)
	0	0.615	2.78	69.0	1.18
WQ-1	0.5 equiv	0.662	4.10	69.5	1.89
	1.0 equiv	0.586	3.19	69.1	1.29
	0	0.580	3.99	68.40	1.58
WQ-2	0.5 equiv	0.612	5.51	66.74	2.25
	1.0 equiv	0.610	4.86	67.30	1.99

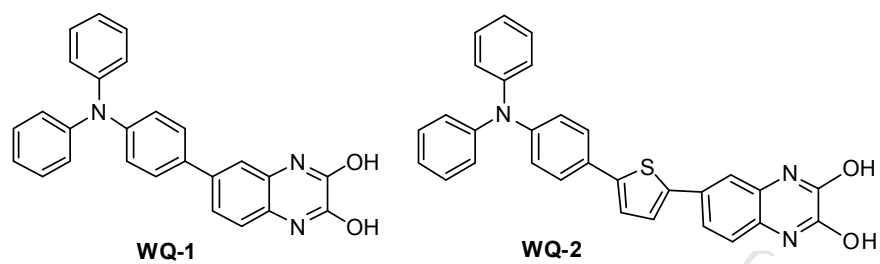
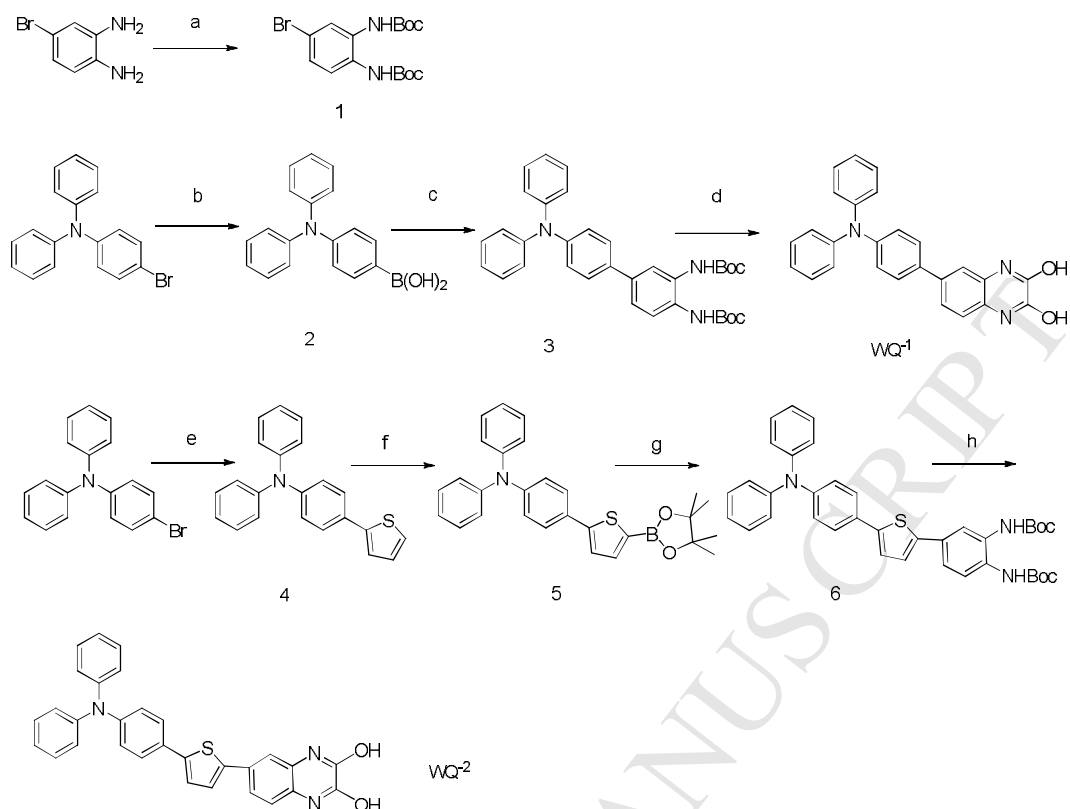


Figure 1 The structures of dyes **WQ-1**, **WQ-2**



(a) di-tert-butyl dicarbonate, r.t., 8 h; (b) (1) nBuLi, THF, -78 °C, 1 h; (2) B(OMe)₃, -78 °C, 1 h; (3) HCl, 0.5 h; (c) **1**, di-tert-butyl (4-bromo-1,2-phenylene)dicarbamate, Pd(PPh₃)₄, K₂CO₃ (2 M), THF, 70 °C, overnight; (d) (1) trifluoroacetic acid, CH₂Cl₂, r. t. , 4 h; (2) oxalic acid dihydrate, 170 °C, 6 h; (e) 2-thiopheneboronic acid, Pd(PPh₃)₄, K₂CO₃ (2 M), THF, 70 °C, overnight; (f) (1) nBuLi, THF, -78 °C, 1 h; (2) 2-isopropoxy-4,4,5,5-tetramethyl-1,3,2-dioxaborolane, -78 °C, 1 h; (g) **1**, trifluoroacetic acid, CH₂Cl₂, r.t., 4 h; (h) (1) trifluoroacetic acid, CH₂Cl₂, r. t. , 4 h; (2) oxalic acid dihydrate, 170 °C, 6 h.

Scheme 1 Synthetic routes of **WQ** dyes

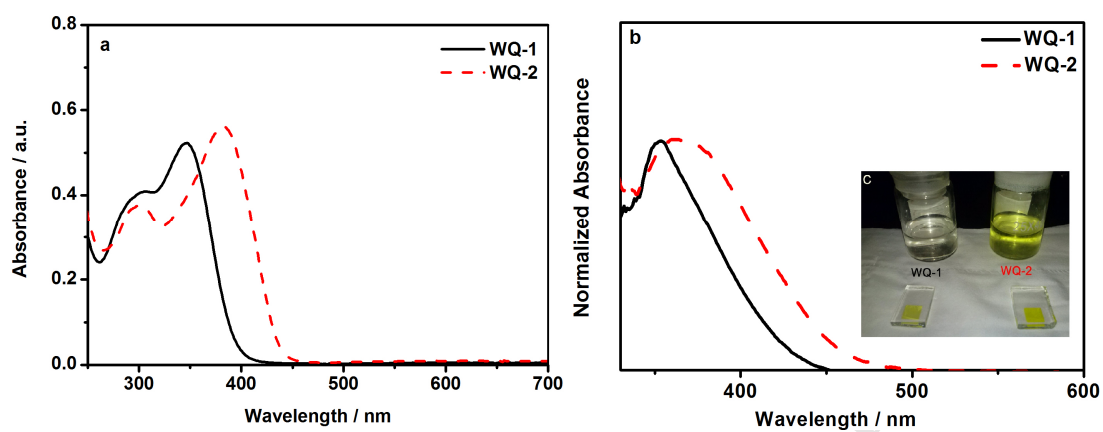


Figure 2 The absorption spectra of **WQ-1**, **WQ-2** in ethanol and dichloromethane (v/v, 4/1) solution (a) and on the TiO₂ films (b); inset is the photograph of the solutions and films (c)

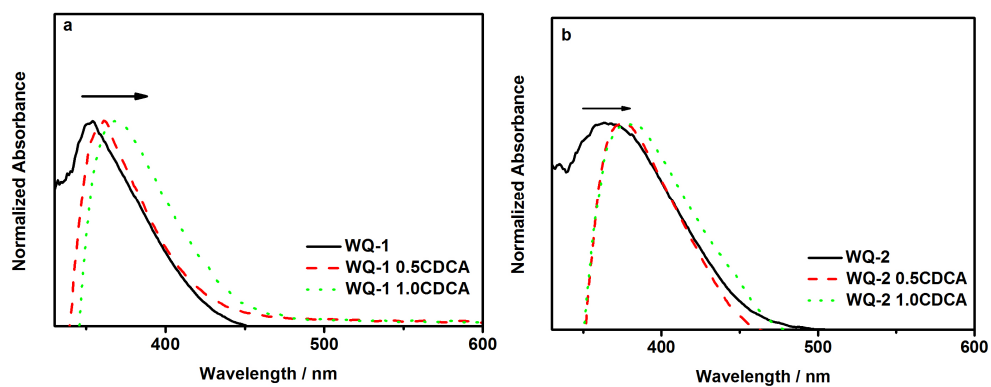


Figure 3 The absorption spectra of **WQ-1** (a), **WQ-2** (b) on the films co-sensitized with CDCA

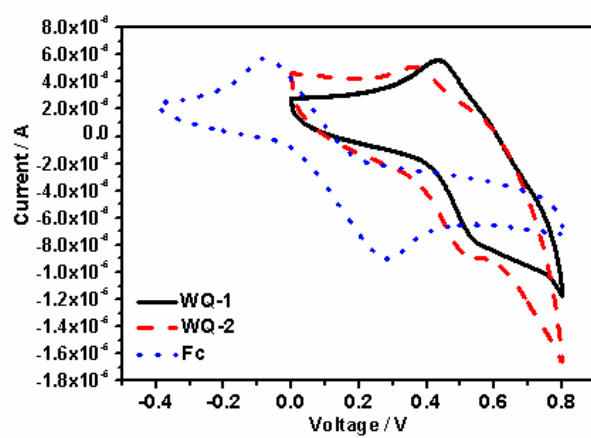


Figure 4 CV curves of WQ dyes

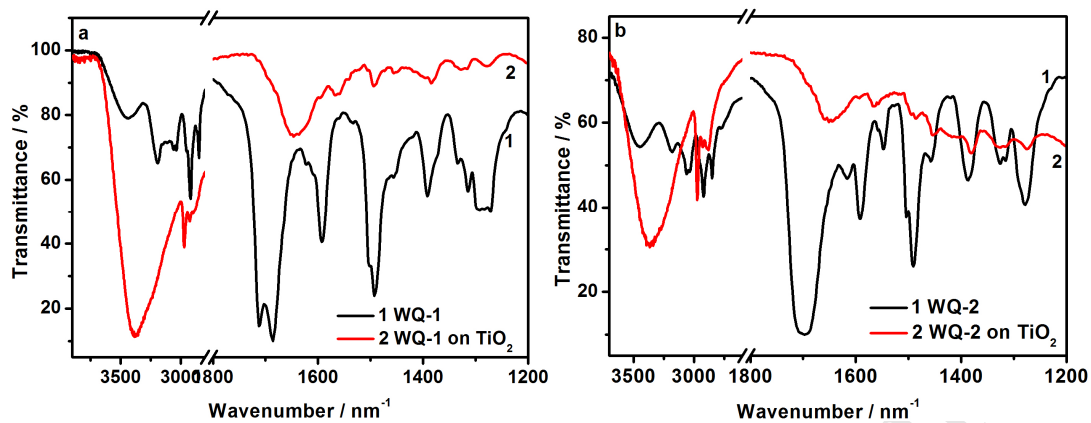


Figure 5 FTIR spectra of WQ-1 and WQ-2 dye powder and dye on the TiO₂

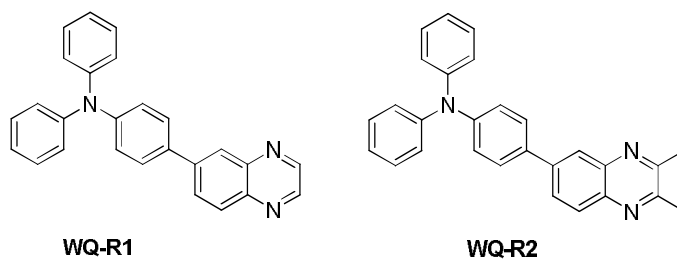


Figure 6 The structures of reference dyes **WQ-R1**, **WQ-R2**

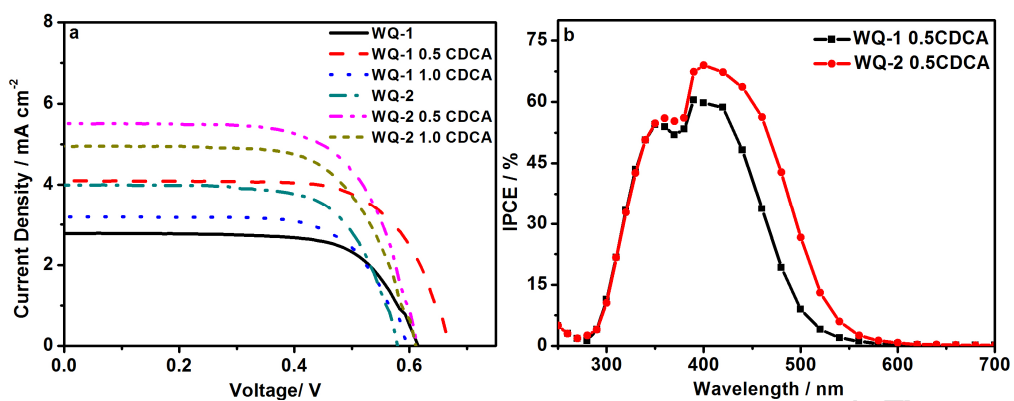


Figure 7 The J - V curves (a) and IPCE spectra (b) of DSSCs based on **WQ-1**, **WQ-2** dyes

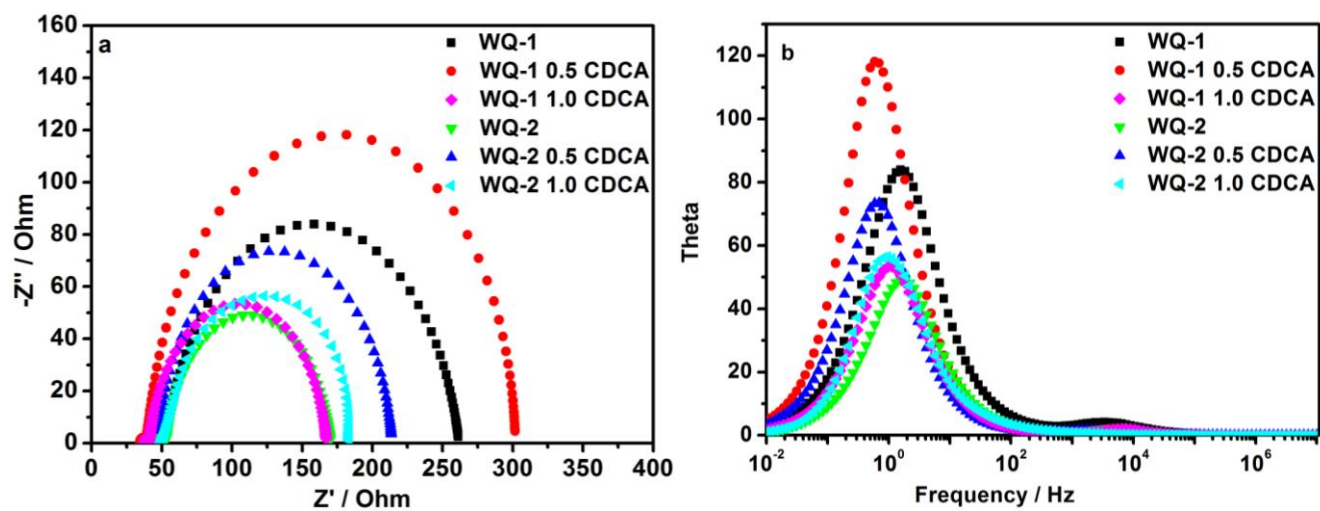


Figure 8 The Nyquist (a) and Bode (b) plots of DSSCs based on **WQ-1** and **WQ-2**

Highlights

1. Organic dye-sensitizers with new anchoring group for the application in DSSCs.
2. The new anchoring group has a structure of quinoxaline-2, 3-diol.
3. The adsorption state of the dye series was studied by FTIR and ascertained by reference dye molecules.

Supporting Information

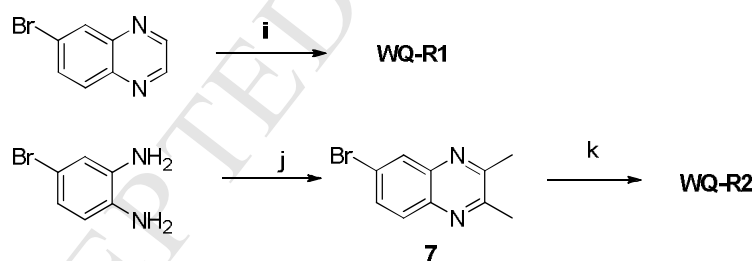
Novel Organic Dyes with Anchoring Group of Quinoxaline-2, 3-diol and the
Application in Dye-sensitized Solar Cells

Lei Wang,^a Xichuan Yang, *^a Xiuna Wang^a and Licheng Sun^{a, b}

^a State Key Laboratory of Fine Chemicals, Dalian University of Technology (DUT),
DUT-KTH Joint Education and Research Center on Molecular Devices, Dalian
116024, China.

^b Department of Chemistry, School of Chemical Science and Engineering, KTH Royal
Institute of Technology, 100 44 Stockholm, Sweden.

* E-mail: yangxc@dlut.edu.cn; Fax: (+86) 411-84986250



(i) **2**, Pd(PPh₃)₄, K₂CO₃ (2 M), THF, 70 °C, overnight; (j) biacetyl, methanol, r.m., 5 h; (k) **2**, Pd(PPh₃)₄, K₂CO₃ (2 M), THF, 70 °C, overnight

Scheme.S1 Synthetic routes of reference dyes.

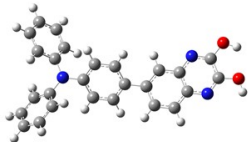
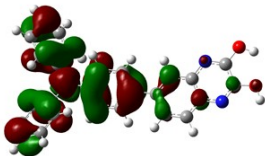
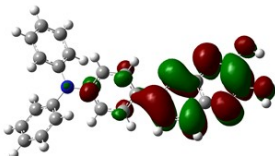
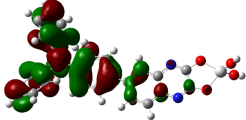
6-bromo-2, 3-dimethylquinoxaline (7): biacetyl (173 mg, 2 mmol) and 4-bromobenzene-1, 2-diamine (374 mg, 2mmol) were added into 15 ml EtOH and stirred for 5 h at r.m.. The solvent was then evaporated and the crude product was purified by column chromatography using CH₂Cl₂ to get compound **7** as a white solid (379 mg, yield 80%). **7**: ¹H NMR (400 MHz, CDCl₃) δ 8.17 (d, *J* = 2.1 Hz, 1H), 7.86 (d, *J* = 8.9 Hz, 1H), 7.75 (dd, *J* = 8.9, 2.1 Hz, 1H), 2.73 (d, *J* = 5.4 Hz, 6H). TOF HRMS calcd. for C₁₀H₉N₂Br [M⁺] 235.9952, found 235.9949.

WQ-R1: 6-bromoquinoxaline and compound **2** were reacted as reaction c to get the yellow solid **WQ-R1**. **WQ-R1**: ¹H NMR (400 MHz, CDCl₃) δ 8.84 (dd, *J* = 15.4, 1.8 Hz, 2H), 8.28 (d, *J* = 1.9 Hz, 1H), 8.15 (d, *J* = 8.8 Hz, 1H), 8.05 (dd, *J* = 8.8, 2.0

Hz, 1H), 7.69 – 7.59 (m, 2H), 7.31 (dd, $J = 11.1, 4.7$ Hz, 4H), 7.19 (dd, $J = 11.8, 4.8$ Hz, 6H), 7.08 (t, $J = 7.3$ Hz, 2H). TOF HRMS calcd. for $C_{26}H_{19}N_3$ [M⁺] 373.1578, found 373.1579.

WQ-R2: Compound 7 and compound 2 were reacted as reaction **c** to get the yellow solid **WQ-R2**. **WQ-R2:** 1H NMR (400 MHz, $CDCl_3$) δ 8.20 (s, 1H), 8.04 (d, $J = 8.7$ Hz, 1H), 7.95 (dd, $J = 8.7, 1.9$ Hz, 1H), 7.66 – 7.58 (m, 2H), 7.32 – 7.27 (m, 4H), 7.21 – 7.14 (m, 6H), 7.07 (t, $J = 7.3$ Hz, 2H), 2.77 (d, $J = 2.8$ Hz, 6H). TOF-HRMS calcd. for $C_{28}H_{23}N_3$ [M⁺] 401.1886, found 401.1892.

Table S1 The optimized structures and electron distribution in HOMO and LUMO levels of the **WQ-1**, **WQ-2** dyes

Dye	Optimized Structure	HOMO	LUMO
			
WQ-1			
WQ-2	